

## Supplementary Methods

### Nanomaterial

The ENM used in this study, namely SAS NM-200 (further renamed as JRCNM02000a)<sup>S1</sup>, was provided by the European Commission Joint Research Center (JRC), Institute for Health and Consumer Protection, Nanomaterials Repository (Ispra, Italy) in the framework of the OECD sponsorship program as a representative SiO<sub>2</sub> nanomaterial. It is an industrially manufactured, precipitated SAS with a primary particle size around 20 nm, mainly used for food processing. The main characteristics of NM-200 (further renamed as JRCNM02000a) are summed up in Table S1.

**Table S1. Main physicochemical characteristics of SAS NM-200<sup>a</sup>.**

ENM-code	Production method	Powder				Batch dispersion <sup>e</sup>		
		Primary particle size <sup>b</sup> (nm)	Particle size distribution (nm)	Purity <sup>c</sup> (wt %)	Main impurities <sup>c</sup> (wt %)	BET SSA <sup>d</sup> (m <sup>2</sup> /g)	Z-average <sup>f</sup> (nm)	Polydispersity index <sup>f</sup>
NM-200	Precipitation	14-23	<100: 89% <50: 70 % <10: 2 %	96.5	Na (0.88) S (0.46) Al (0.87)	189.2	185±15	0.313±0.023

<sup>a</sup> JRC-Nanomaterials-Repository, 2016; Rasmussen et al., 2013

<sup>b</sup> Determined by transmission electron microscopy

<sup>c</sup> Determined by energy dispersive spectrometry

<sup>d</sup> BET (Brunauer-Emmet-Teller) specific surface area (SSA). Determined by nitrogen adsorption

<sup>e</sup> Stock suspensions prepared according to the Nanogenotox dispersion protocol

<sup>f</sup> Determined by dynamic light scattering

### Preparation of the stock suspensions of NM-200

Stock suspensions of NM-200 were prepared using the standardized dispersion protocol developed in the Nanogenotox Joint Action ([www.nanogenotox.eu](http://www.nanogenotox.eu))<sup>S2, S3</sup>. This standard operation procedure was established in order to harmonize and standardize the dispersion of ENMs for *in vitro* and *in vivo* toxicity testing. Briefly, NPs were suspended in sterile-filtered 0.05% w/v BSA-water at a concentration of 2.56 mg/mL using high energy probe sonication at 4°C. In these conditions dispersions are dominated by a mode with a peak-size slightly smaller

than 100 nm and a second smaller mode (by number) at ca. 30 to 40 nm<sup>S3</sup>. Dispersions have a tail upwards, due to the presence of coarse particles (in the size range of hundreds of nanometers)<sup>S3</sup>. The corresponding average zeta-size and polydispersity index of the size spectra are listed in Table S1 (see ‘Batch dispersion’). The pH value of dispersions was 7 in all cases.

### **Particle size distribution of the final suspension of NM-200**

Freshly dispersed, the NM-200 stock suspension was used to prepare a drinking solution to reach a final concentration of 30 mg NM-200/L. This concentration results in a mice exposure of about 2 mg NM-200/kg bw/day that is in the range of the estimated human daily exposure to silicon dioxide for the nanofraction. The particle size distribution of the final suspension administered to mice was characterized by asymmetric flow-field flow fractionation (FFF) coupled on line to ICP-MS/MS. The asymmetric flow FFF system consisted of a metal-free AF2000 MT model (Postnova Analytics, Landsberg am Lech, Germany), equipped with a flat separation channel (320 mm × 60 mm) of 280 mm length. A 350- $\mu$ m spacer was used along with a 10 kDa molecular weight cutoff regenerated cellulose membrane (Lot. CF 071113-0613 14439 Postnova Analytics) as accumulation wall. Manual injection was performed using a 50- $\mu$ l loop. The carrier liquid consisted of a 0.22- $\mu$ m filtered mixture containing (NH<sub>4</sub>)<sub>2</sub>CO<sub>3</sub> 0.25 mM.

ICP-MS detection was performed using an ICP-QQQ mass spectrometer (Agilent 8800, Agilent Technologies Inc., Tokyo, Japan) equipped with an octopole-based collision/reaction cell (ORS<sup>3</sup> Cell) in-between the two quadrupole analyzers (Q1 and Q2) and operated in MS/MS mode using O<sub>2</sub> (5.0 purity grade) as reaction gas. Operating conditions have been previously reported<sup>S4</sup>.

Near-monodisperse non-functionalized silica nanoparticle suspensions ('NanoXact') with nominal diameters of 20, 50, 80, 100, 120, 160, and 200 nm obtained by Nanocomposix (San Diego, CA) were used for system size calibration to convert retention time ( $t_r$ ) into hydrodynamic diameter ( $d_h$ ). The particle size distribution of the NM-200 dispersion administered to mice showed the presence of a major peak at  $112.8 \pm 6.1$  nm and a minor one at  $140.8 \pm 1.4$  nm.

### **Selection of NM-200 delivery through drinking water**

Owing to the duration of the study, (18 months), exposure through drinking water was selected rather than a daily intra-gastric administration or administration through food pellet. Drinking water offers the advantage of a regular spread out over the day, without any special handlings of the animals. Even though the exact dose delivered cannot be calculated with the same accuracy of the intra-gastric administration, a realistic estimate of the daily intake is possible with the advantage of performing long-term repeated exposure (continuous, for 18 months).

### **Estimation of mouse daily intake**

In the mouse, the average daily water intake is estimated to be around 3-5 mL (1.5 mL/10 g body weight/day) (<http://web.jhu.edu/animalcare/procedures/mouse.html>). In the present study, the usual estimated individual intake of 4 mL/day was used to calculate the average daily intake of mice. Therefore, the mean administered dose over the entire experiment duration was estimated to be 4.8 mg SiO<sub>2</sub>/kg body weight/day ( $30 \mu\text{g/mL} \cdot 4 \text{ mL} = 120 \mu\text{g}$  per day/per mouse, for an average weight of 25 g,  $120 \mu\text{g} / 25\text{g} = 4.8 \mu\text{g/g}$  bw/per day, i.e. 4.8 mg/Kg bw/ per day).

### **Study design**

The experimental design is summed up in Figure S1.

## EXPERIMENTAL DESIGN

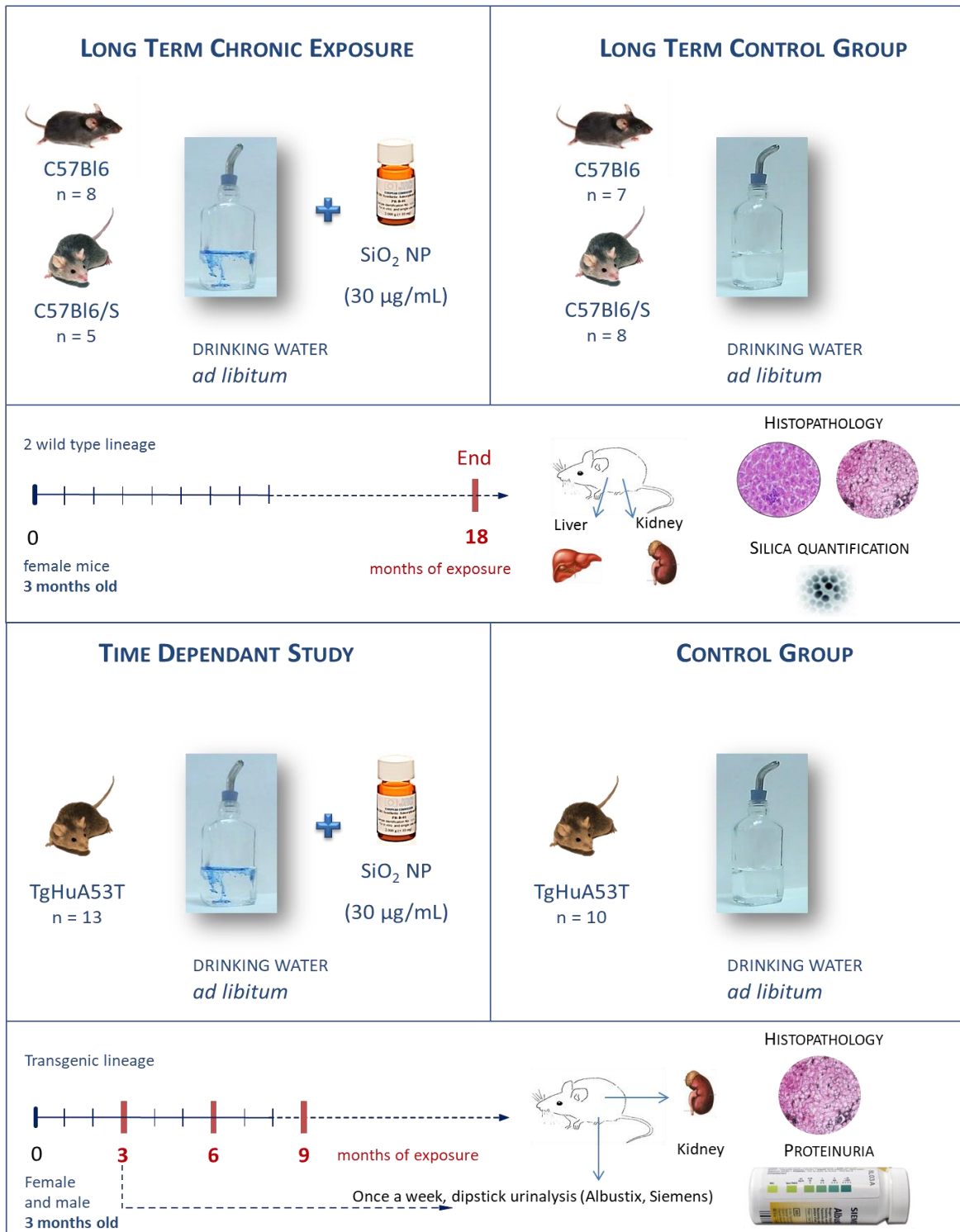


**Figure S1.** Schematic view of the experimental design. The impact of 18-month exposure to SiO<sub>2</sub> NPs through drinking water in wild type mice was studied. Besides, a time dependent study was performed in the TgHuA53T transgenic mouse line in order to assess the effects of 3, 6 and 9 months exposure to silica in drinking water.

The animals were housed in a controlled environment at a temperature of 22 to 24 °C, humidity of 45-65 % and 12 h light/dark cycle. Food and drinking water were given *ad libitum*. All the animals (exposed or not) were fed with a commercial complete diet (Mucedola, Milan, Italy, 4RF25 and 4RF21).

Based on previous experience of long term neurodegenerative studies in mouse, we chose two wild-type mouse lines, C57BL/6 mice (Charles River, France) and C57BL/6S mice<sup>S5</sup> (Harlan, France), the latter presenting a spontaneous deletion of the  $\alpha$ -syn locus and that is currently used as negative control in  $\alpha$ -synucleinopathies (e.g. Parkinson disease) experiments. A control group of each mouse line ( $n=7$  and  $n=8$ ) received only tap water during the 18 months of the experiment, in order to get aged-control cases. Exposed groups consisted in 5 to 8 female mice, 3-month-old at the beginning of the experiment (average weight 20 to 25 g), exposed orally to NPs through their drinking water for 18 months.

Besides, a third experiment was set up after the main study using a transgenic mouse model, expressing the human mutated (A53T)  $\alpha$ -synuclein protein (TgHu53T)<sup>S6, S7</sup>. This transgenic mouse model of human synucleinopathy overexpresses A53T mutant human  $\alpha$ -syn under a prion promoter (B6; C3H-Tg(SNCA)83Vle/J). Homozygous TgHu53T male and female mice (produced in Anses Lyon approved animal facilities PFEA) were used in order to study the impact of 3, 6 and 9 months exposure to silica in drinking water on young (8 weeks old, average weight 20 to 25 g) transgenic mice ( $n = 15$ , male and female) compared to the matched controls ( $n= 10$  unexposed transgenic mice).

A novel NP stock suspension was prepared each week; once freshly dispersed, it was diluted with tap water to reach a final concentration of 30 mg NM-200/L. The resulting NP dispersion was given as drinking water to mice and was changed as usually, i.e. twice a week. Monitoring

of stress, morbidity, mortality, was accurately performed twice a week during the change of feed, water and litter.

### **Liver preparation for histopathology**

Liver samples, fixed in 10% buffered formalin solution, were embedded in paraffin. Sections (5- $\mu$ m-thick) were stained with hematoxylin-eosin and Red Congo. Histopathological changes in the liver parenchyma (- cytoplasmic vacuolization and nuclear atypia in hepatocytes, extramedullary hematopoiesis and megacaryocytes, portal and lobular inflammation, vascular and sinusoidal abnormalities), as well as the amyloidosis status were examined by a hepatopathologist on sections stained with hematoxylin-eosin and Red Congo, respectively. Steatotic-like cytoplasmic vacuolization and inflammation were semi-quantified as 0 (absent), + (minimal) and ++ (marked) for cytoplasmic vacuolization, and 0/(+) (absent or not more than one inflammatory foci without apoptotic body and without more than ten inflammatory cells in the overall cut section), + (few inflammatory foci) and ++ (numerous inflammatory foci) for inflammation.

### **Kidney preparation for histopathology**

Kidney preparation consisted in a first sagittal bisection to allow specific stainings on resin and frozen sections. After a first fixation step in a sodium cacodylate-glutaraldehyde 4% buffer during 15 min, first halves of kidneys were fixed overnight in Japanese fixator (3% PFA, 2% sodium cacodylate and 0.2% of picric acid), then rinsed in 3 baths (5 min each) of sodium cacodylate and dehydrated in 2 acetone baths (60 min each). Samples were then impregnated during 4 hours at 4°C in glycolmethacrylate (GMA) and finally embedded in resin (GMA and aniline/propanol solution) at 4°C until resin polymerization. Sagittal sections (0.5 to 3- $\mu$ m-thick) representative of the whole kidney, were cut from resin blocks with a microtome (Leica Jung Supercut 2065®) and deposited on treated slides (Superfrost plus, Thermo-Scientific).

The other half kidneys, previously included in a cryopreservative solution (Tissue-Tech®: Sakura, Netherlands) and frozen in liquid nitrogen ( $-196^{\circ}\text{C}$ ) were used to characterize in depth findings suggestive of amyloidosis. Four  $\mu\text{m}$ -thick sagittal frozen sections (Leica CM 3000® cryostat), collected on Superfrost plus slides, were either stained with Cristal Violet or Congo Red or used for immunofluorescence (IF) study. Briefly, after 20 min of fixation using acetone (Sigma, France), slides were placed in a humidified chamber for 30 min in the dark with the appropriate antibody solution - antibodies against IgM, IgG, kappa and lambda chains, beta amyloid protein - according to the manufacturer's instructions (Abcam, France), and recapitulated in Table S2.

**Table S2. List of antibodies used for amyloidosis characterization by immunohistochemistry.**

Antibodies	Supplier (catalog number)	Dilution
$\beta$ amyloid protein unconjugated (rabbit polyclonal)	Abcam, ab10148	1/50
Goat anti-mouse IgG, Alexa fluor 488	Abcam, ab150117	1/400
Goat anti-mouse IgM, Alexa fluor 488	Abcam, ab150121	1/500
K light chain, FITC	Abcam, ab99615	1/400
$\lambda$ light chain, FITC	Abcam, ab99623	1/400
Secondary Goat anti-rabbit IgG fluorescent	Abcam, ab6717	1/500
Mouse Serum Amyloid A1/A2 (SAA) (goat polyclonal)	R&D Systems, AF2948	1/500
Secondary rabbit anti-goat	Jackson immunoResearch laboratories, ref 305-005-045	1/400

Primary antibodies were directly conjugated (FITC or Alexa fluor 488) except for the anti-amyloid protein antigen (unconjugated); for the latter, after  $3 \times 10$  min PBS baths (BioMérieux, France), a specific goat anti-rabbit FITC antibody (Abcam, France) was applied for 30 min in

the dark. Then, slides were thoroughly rinsed in PBS baths before mounting with a specific fluorescent medium (Dako, France). Replacement of the primary antibody by PBS was used as internal IF negative control.

Liver and kidney sections (5- $\mu$ m-thick) from remaining tissue blocks (post fixed in 10% buffered formalin solution, embedded in paraffin) were also used to test SAA. For that purpose, immunohistochemistry was performed by the Pathology Research Platform, Department of Translational Research and Innovation, (Centre Léon Bérard, Lyon, France), on an automated immunostainer (Ventana Discovery XT, Roche, Meylan, France) using Omnimap DAB Kit according to the manufacturer's instructions. Once routinely deparaffinized, sections were treated in order to unmask antigenic sites in a CC1 buffer (Roche, EDTA pH8-8.5) at 95°C for either 36 or 20 min. The sections were incubated with the goat anti mouse anti serum amyloid (SAA) diluted at 1/500, in a diluting solution MM France (F/936B-08 Antibody Diluent EMERALD). Then the secondary antibodies, a rabbit anti-goat, were applied at 1/400. The Omnimap rabbit kit from Roche, ready to use, was applied for 16 min, and the staining was visualized with 3,3'-diaminobenzidine (DAB) as a chromogenic substrate (Kit chromo map Roche (DAB 8 min)). Finally, the sections were counterstained with Gill's hematoxylin. Validation and calibration of the staining were performed using biospecimens without amyloid and with amyloid. Replacement of the primary antibody by the diluting solution (Antibody Diluent EMERALD) was used as internal immunohistochemical negative control. Staining was pretreatment dependent. Without unmasking steps, no staining is observable whatever the concentration used. Among the different dilutions tested, 1/50, 1/200 and 1/500, the highest dilution offered the best specific signal detection, the others leading to obvious saturated signals.



### **Total silicon determination in tissues**

All procedures were carried out under clean room conditions to avoid any contamination. Organs were placed in high-pressure Teflon containers with a 10:1 and 2:1 volume to weight ratio of HNO<sub>3</sub> and HF (ultrapure grade, Carlo Erba, Rodano, Italy), respectively. Samples were digested in a microwave system (UltraWAVE Single Reaction Chamber Microwave Digestion System, Milestone, Bergamo, Italy) with the following program: 23 min at 220 °C (ramp), 10 min at 220 °C (hold, maximum power 1400 W), 15 min of depressurization and cooling at room temperature. Total silicon concentrations were determined by means of an Agilent 8800 ICP-QQQ mass spectrometer. The sample introduction system of the ICP mass spectrometer was replaced with inert (non-quartz) components, i.e. a platinum injector and a PFA concentric nebulizer with a double-pass PFA spray chamber cooled to 2°C. Optimized analytical conditions for accurate Si detection by ICP-MS/MS have been reported elsewhere <sup>S4</sup>. Quantitative determinations were carried out by the method of standard addition. Trueness was assessed by the analysis of the internal quality control material ISS-BL, a bovine liver sample spiked with soluble silicon, with a reference value for Si of 20.4 ± 1.9 µg/g <sup>S8</sup>, which was included in each analytical batch. The average determined Si concentration was 19.1 ± 1.7 µg/g (n = 4), in good agreement with the target value.

### **Statistical analyses**

Statistical analyses for tissue silicon content were carried out comparing exposed to control groups by means of the Mann-Whitney U test. The association between group and the amount of protein in urine was evaluated by the chi-squared test. A proportion test was performed to compare the amount of protein in control and NM 200 SiO<sub>2</sub> group urine for each level. A *p* value <0.05 was considered statistically significant. Statistical analyses were performed by SPSS Statistics version 25 for Windows (SPSS Statistics, IBM Corp.).

## Supplementary Data Set

### Histopathological changes in livers from NM-200 exposed mice

The histopathological alterations, illustrated in Figure S2, are summarized in Table S3

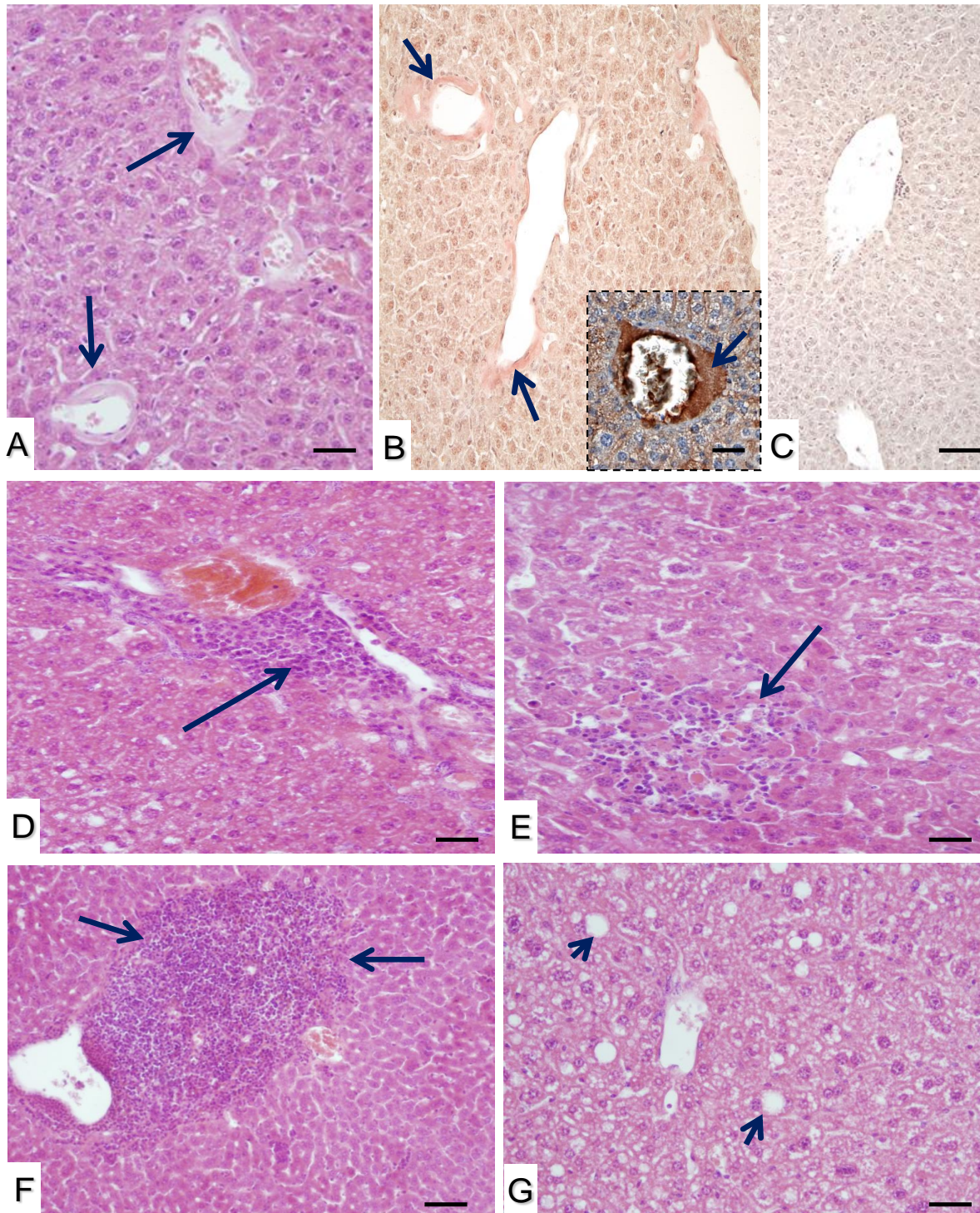


**Figure S2. Histopathological changes in livers from NM-200 exposed mice**

A and B. Perivascular amyloid deposition (arrows) in the liver parenchyma of 3 of 7 C57BL/6 mice exposed to SAS NP – Positively labeled using a murine anti-SAA antibody (insert in B,

brown deposits). Absence of deposition in controls (C), represented by unexposed C57BL/6 aged-matched mice (A: H&E stain; B and C; Congo red stain; D, E, F: H&E stain). In SAS NP exposed animals, few mononuclear inflammatory infiltrates mainly composed of small lymphocytes were scarcely dispersed in portal areas (D, arrows) and/or in lobular areas (E, arrows). Larger nodular lymphoid infiltrates (F, arrows) were seen in portal tracts of one C57BL/6 mouse exposed to SAS NP. G (H&E stain): Steatotic-like cytoplasmic vacuolization

**Table S3: Summary of the histopathological changes observed in the liver of mice after 18-month exposure to SAS NM-200 via drinking water. The lesion scoring was recorded using a 3 grade system 0 (absent), + (minimal), and ++ (marked). Steatotic-like cytoplasmic vacuolization and inflammation were semi-quantified as 0 (absent), + (minimal) and ++ (marked) for cytoplasmic vacuolization, and 0/(+) (absent or not more than one inflammatory foci without apoptotic body and without more than ten inflammatory cells in the overall cut section), + (few inflammatory foci) and ++ (numerous inflammatory foci) for inflammation.**

		<b>LIVER HISTOPATHOLOGICAL CHANGES</b>					
<b>EXPOSURE</b>	<b>MOUSE LINE</b>	<b>AMYLOID STATUS</b>	<b>CYTOPLASMIC VACUOLIZATION</b>	<b>PORTAL LYMPHOID INFILTRATES</b>	<b>LOBULAR LYMPHOID INFILTRATES</b>	<b>MEGACARYOCYTES</b>	<b>BLOOD VESSELS</b>
Control group exposed to tap water without NPs	<b>C57BL/6S (n=8)</b>	No abnormalities	+ (4/8) ++ (2/8)	+ (3/8)	+ (3/8)	+ 1/8	No abnormalities
	<b>C57BL/6 (n=2) age matched and (n=7) young adult</b>	No abnormalities	0	0	+ (1/9) in aged matched	None	No abnormalities
<b>SiO<sub>2</sub>-NPs</b>	<b>C57BL/6S (n=5)</b>	No abnormalities	+ (2/5) ++ (3/5)	0 or (+)	+ (3/5)	+ 3/5	+ 1/5 Sinusoidal dilatation
	<b>C57BL/6 (n=6)</b>	+ 3/6 Perivascular amyloid deposition	0	+ (2/6) ++ (1/6)	+ (2/6)	None	+ 2/6 Sinusoidal dilatation

In liver parenchyma (Figure S2) perivascular amyloid accumulation was only observed in C57BL/6 mice (3/7). These amyloid deposits were detected as SAA immunoreactive (see insert Fig S2 B). This observation combined to the SAA amyloidosis observed in the kidney (1/3) (Figure S2 A, B) examined in the same group could be considered not as a chance finding but more likely as related to the treatment. Small inflammatory infiltrates were scarcely dispersed in the liver parenchyma, whatever the condition was (Figure S2 C, D). They mostly corresponded to foci of small lymphocytes in portal spaces and in lobules where they were associated to occasional apoptotic bodies into necro-inflammatory lesions. Larger nodular lymphoid infiltrates were observed in portal areas of one C57BL/6 mouse exposed to SAS NM-200 (Figure S2 E). Finally, hepatocytes from mice deleted for  $\alpha$ -synuclein displayed steatotic-like cytoplasmic vacuolization (micro- or macro vacuoles similar to those observed in human steatosis), independent of their exposure to SAS NM-200 (Figure S2 F).

### Tissue Si deposition in transgenic mice

Silicon levels in kidneys of treated TgHuA53T transgenic mice were higher than controls (Figure S3,  $p < 0.05$ ). Levels at month 6 were lower than month 3, which may be due to redistribution of silica to other tissues.

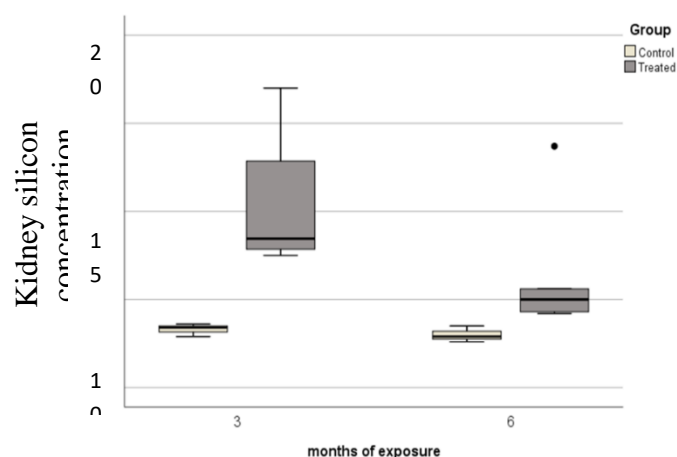


### Figure S3. Tissue Si deposition in transgenic mice

Silicon concentrations ( $\mu\text{g Si/g}$  of fresh tissue) in kidneys of treated TgHuA53T transgenic mice at month 3 and 6 ( $n=3-5$ ).

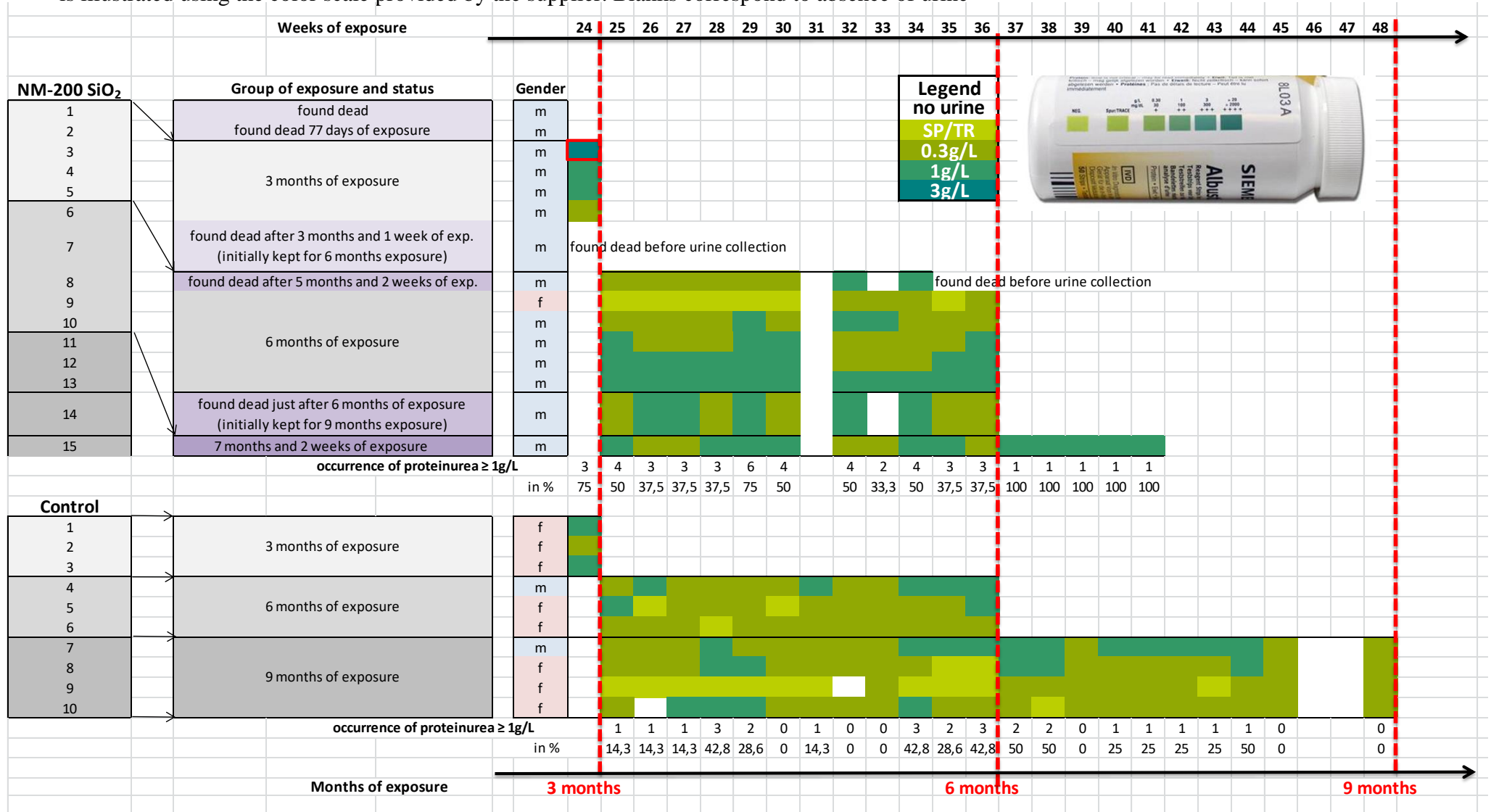
## **Proteinuria and Histopathological changes in kidneys from NM-200 exposed transgenic mice**

At the time the study on wild type mice was designed, adverse effects on kidney function were unforeseen and this endpoint was not evaluated. However, when the first histopathological observations were made, a urine test was set up for the latest ongoing experiment on transgenic mice expressing the human mutated (A53T)  $\alpha$ -synuclein protein. Proteinuria was monitored weekly by dipstick urinalysis (Albustix, Siemens) - from the 3<sup>rd</sup> month of exposure - and results are provided in Table S4.

Using the colored scale of the test used, the table shows variations all along the weeks. The rate of 1 g/L revealing a clear proteinuria was more frequent in exposed mice - 38 to 75% - compared to controls - 0 to 43% - for the available data collected between 3<sup>rd</sup> and 6<sup>th</sup> month of exposure ( $p < 0.001$ ). Mice from exposed groups showed once a rate of 3 g/L which is pathological and indirectly reflects a severe renal insufficiency.



**Table S4. Proteinuria changes in kidneys from NM-200 exposed transgenic mice.** Proteinuria monitored weekly by dipstick urinalysis (Albustix, Siemens) from the 3rd month of experiment in TgHuA53T mice exposed or not to NM 200 SiO<sub>2</sub> by oral route. The amount of protein in urine detected is illustrated using the color scale provided by the supplier. Blanks correspond to absence of urine



In control groups, histopathological analysis of the kidneys revealed no lesion (figure S4 A&B). In the exposed group, after 3 months of exposure, histopathological analysis of the kidneys revealed no lesions and absence of amyloid deposit; additionally premature deaths of 3 TgM83mice exposed to SiO<sub>2</sub> did not allow to test proteinuria, nor kidney histopathology. After 6 months of exposure, tubular lesions were present in the kidneys with many vacuoles (figure S4 C-D) that suggest possible toxicity. Proteinuria suggests glomerular dysfunction without significant glomerular amyloidosis alterations at this stage. Several cases of unexpected death were observed (6 males and only in the exposed group). These animals died before the 6<sup>th</sup> month of exposure except one that died at 7 months and one week of exposure with a 1 g/L proteinuria (illustrated in figure S4C). Therefore, effects of longer exposure (9 months) could not be studied.

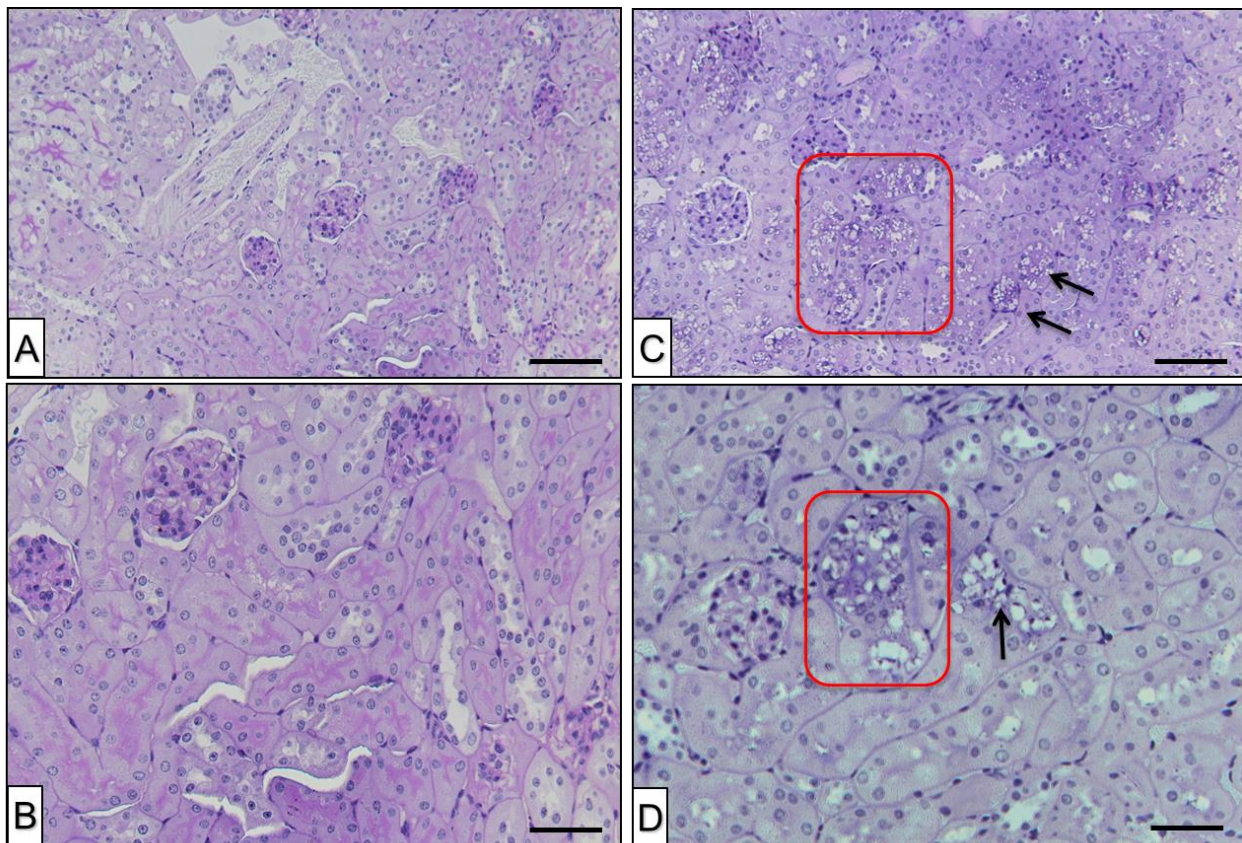


**Figure S4. Histopathological changes in kidneys from NM-200 exposed transgenic mice.** A-D H&E stain of kidneys from TgHuA53T mice. A-B kidney from control group shows no abnormalities on glomerulus or tubules whatever the age studied. On the contrary, after 6 months of exposure to NM-200, many vacuoles were detected in tubules (arrows and surrounded areas) of TgHuA53T mice without



atrophic lesions or tubular necrosis (C and D, at higher magnification). Scale bars: 200  $\mu\text{m}$  for A-C, 100  $\mu\text{m}$  for B-D.

## Supplementary References

- S1. JRC-Nanomaterials-Repository: List of Representative Nanomaterials. In [http://ihcp.jrc.ec.europa.eu/our\\_activities/nanotechnology/nanomaterials-repository](http://ihcp.jrc.ec.europa.eu/our_activities/nanotechnology/nanomaterials-repository), 2016.
- S2. Schmid K, Riediker M. Use of nanoparticles in Swiss Industry: a targeted survey. *Environmental science & technology* 2008; 42: 2253-2260.
- S3. Jensen KA, Kembouche Y, Christiansen E, *et al.* Web-Report : The generic NANOGENOTOX dispersion protocol – Standard Operation Procedure (SOP). 2011.
- S4 Aureli F, D'Amato M, Raggi A, *et al.* Quantitative characterization of silica nanoparticles by asymmetric flow field flow fractionation coupled with online multiangle light scattering and ICP-MS/MS detection. *Journal of Analytical Atomic Spectroscopy* 2015; 30: 1266-1273.
- S5. Specht CG, Schoepfer R. Deletion of the alpha-synuclein locus in a subpopulation of C57BL/6J inbred mice. *BMC Neurosci* 2001; 2: 11.
- S6. Giasson BI, Duda JE, Quinn SM, *et al.* Neuronal alpha-synucleinopathy with severe movement disorder in mice expressing A53T human alpha-synuclein. *Neuron* 2002; 34: 521-533.
- S7. Bencsik A, Muselli L, Leboindre M, *et al.* Early and persistent expression of phosphorylated alpha-synuclein in the enteric nervous system of A53T mutant human alpha-synuclein transgenic mice. *J Neuropathol Exp Neurol* 2014; 73: 1144-1151.
- S8. Aureli F, D'Amato M, Raggi A, *et al.* Determination of total Si and SiO<sub>2</sub> particles using an ICP-MS based analytical platform for toxicokinetic studies of nanosilica. *In preparation* 2019.